ELSEVIER

Journal of Organometallic Chemistry 660 (2002) 43–49

Journal of Organometallic Chemistry

www.elsevier.com/locate/jorganchem

Molecular structures of trimeric diphenyltin chalcogenides, $(Ph_2SnE)_3$, E = S, Se, Te

Heike Lange [a], Uwe Herzog [a,*], Uwe Böhme [a], Gerd Rheinwald [b]

[a] *Institut für Anorganische Chemie, TU Bergakademie Freiberg, Leipziger Str. 29, D-09596 Freiberg, Germany*
[b] *Institut für Chemie, Lehrstuhl Anorganische Chemie, TU Chemnitz, Straße der Nationen 62, D-09111 Chemnitz, Germany*

Received 14 February 2002; received in revised form 22 April 2002; accepted 20 May 2002

Abstract

The trimeric diphenyltin chalcogenides $(Ph_2SnE)_3$ (E = S (**1**), Se (**2**), Te(**3**)) have been synthesized by reaction of Ph_2SnCl_2 with Li_2E and characterized by multinuclear NMR spectroscopy (^{1}H, ^{13}C, ^{119}Sn, ^{77}Se and ^{125}Te) as well as crystal structure analyses. The three compounds crystallize in the monoclinic space group $P2_1/n$ and show central six-membered rings Sn_3E_3 in twisted boat conformations. For **1** density functional theory (DFT) calculations at the B3LYP/6-31G* level of theory have revealed the twisted boat conformation as the global minimum. Additionally a boat conformation (+3.4 kJ mol^{-1}) and a chair conformation (+7.9 kJ mol^{-1}) have been calculated. The mutual repulsion of the phenyl rings in the chair conformation is also evident from the increased bond angles of the Sn_3S_3 ring in **1**. © 2002 Published by Elsevier Science B.V.

Keywords: Molecular structures; Trimeric diphenyltin chalcogenides; Twisted boat conformations; DFT calculations

1. Introduction

There is a considerable interest in the chemistry of organotin chalcogenides which arises, in part, from their possible application as precursors in the formation of tin chalcogenides [1], which are semiconductors with band gaps of 1.2 eV (SnS), 0.9 eV (SnSe) and 0.2 eV (SnTe) [2]. Trimeric dimethyl tin chalcogenides have been prepared by reaction of Me_2SnCl_2 with Na_2S [3], H_2Se [4] or NaHTe [5], respectively. In the case of the bulky ^{t}Bu substituents, i.e. $^{t}Bu_2SnCl_2$, the reactions with Na_2E (E = S, Se, Te) yield the dimeric compounds $(^{t}Bu_2SnE)_2$ revealing planar four-membered ring Sn_2E_2 [6].

Five-membered ring compounds $Me_4Sn_2(E)_2SnMe_2$ have been obtained in the reaction of Me_2SnH_2 with elemental E in the presence of dimethylformamide [7]. The molecular structure analysis of the selenium compound has revealed an envelope conformation with the distannane unit and the two selenium atoms in one plane [8].

In contrast, the molecular structure analyses of the six-membered ring compounds $(Me_2SnE)_3$ have shown that the Sn_3E_3 rings have twisted boat conformations. Two modifications of $(Me_2SnS)_3$ have been described, a monoclinic form which is observed by sublimation at 80 °C/14 torr [3] and a tetragonal modification (space group $P4_12_12$, obtained by crystallization from solution) with C_2 symmetry of the molecule [9]. The latter modification has also been observed for the selenium compound [4] while $(Me_2SnTe)_3$ shows almost C_2 symmetry and crystallizes in *Pnma* [5].

$(Ph_2SnS)_3$ (**1**) crystallizes in $P2_1/n$ [10–12], also revealing a central six-membered ring Sn_3S_3 in a twisted boat conformation. Analogous conformations have also been found for the homologous $(Ph_2PbS)_3$ [12] and for *trans*-$(PhMeSiS)_3$ [13], so far the only known crystal structure with an unfused Si_3S_3-ring. The crystal structures of the selenium and tellurium derivatives $(Ph_2SnSe)_3$ (**2**) and $(Ph_2SnTe)_3$ (**3**) have been unknown so far, however the formation of **2** has been described in Ref. [1]. In this work we want to report on the syntheses, NMR data and molecular structures of **1**–**3**. The molecular structure of **1**, determined by X-ray analysis, will be compared with results of density functional

* Corresponding author. Tel.: +49-3731-394-343; fax: +49-3731-394-058

E-mail addresses: heike.lange@chemie.tu-freiberg.de (H. Lange), uwe.herzog@chemie.tu-freiberg.de (U. Herzog).

0022-328X/02/$ - see front matter © 2002 Published by Elsevier Science B.V.
PII: S0022-328X(02)01690-X

theory (DFT) calculations of different conformations of the central Sn_3S_3 ring.

2. Results and discussion

The trimeric diphenyltin chalcogenides **1**–**3** have been prepared according to Eq. (1):

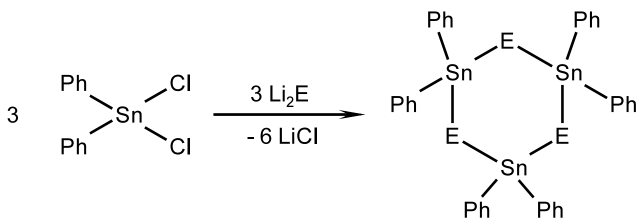

(1)

It had been stated previously that reactions of chlorosilanes and stannanes with commercially available alkali chalcogenides frequently gave very poor yields [1]. Therefore, the applied Li_2E has been prepared in situ from $Li[BEt_3H]$ and the corresponding chalcogen:

$$2\ Li[BEt_3H] + E \xrightarrow{(THF)} Li_2E + 2\ BEt_3 + H_2 \quad (2)$$

The three compounds have been identified by NMR spectroscopy, the observed NMR data including coupling constants are summarized in Tables 1 and 2.

Compared with the NMR data of the corresponding methyl compounds $(Me_2SnE)_3$ [14,15] the ^{119}Sn as well as the ^{77}Se- and ^{125}Te-NMR resonances are shifted to higher field while the coupling constants $^1J_{SnE}$ and $^2J_{SnSn}$ remain almost unchanged (increase by 3–5%), see Fig. 1.

As discussed in Ref. [15] δ_{Te} and $^1J_{SnTe}$ parallel δ_{Se} and $^1J_{SnSe}$ by factors between 2.2 and 2.6. Due to the change from $sp^3 \rightarrow sp^2$ carbon atoms the s bond order and hence the value of the $^1J_{SnC}$ coupling constant increases by a factor of 1.6 from $(Me_2SnE)_3$ to **1**–**3** for the same E, see Table 2 and Ref. [15].

Compounds **1**–**3** could be crystallized from toluene/hexane solutions, and crystal structure analyses were performed from all three compounds, see Figs. 2–4.

The obtained structure of **1** was identical with the one published in Refs. [11,12], but the data were taken at −100 °C like for **2** and **3** exhibiting slightly different cell constants and hence different bond lengths and angles for **1**. All three compounds crystallize in the space group $P2_1/n$, but while **1** and **2** are isomorphous, the orientation of the molecules in the unit cell is different in the tellurium compound **3**, see Figs. 5 and 6. This causes the different orientations of the phenyl rings in **3** in comparison with **1** and **2** (see Figs. 2–4).

All three compounds reveal a central six-membered ring Sn_3E_3 adopting a twisted boat conformation. Selected bond lengths, angles and dihedral angles are summarized in Tables 3–5.

The Sn–E bond lengths are in good agreement with the values found for the corresponding methyl derivatives and close to the calculated bond lengths for Sn–E single bonds, Sn–S: 2.39 Å, Sn–Se: 2.53 Å and Sn–Te: 2.73 Å [16]. The angles Sn–E–Sn are all smaller than the ideal tetrahedral angle and decrease in the order S > Se > Te (average of 104.74, 101.98 and 97.42°). The dihedral angles within the central Sn_3E_3 rings are close to the sequence $+\varphi_1$, $+\varphi_2$, $-(\varphi_1+\varphi_2)$, $+\varphi_1$, $+\varphi_2$, $-(\varphi_1+\varphi_2)$ which would be an ideal twisted boat conformation with C_2 symmetry.

DFT calculations at the B3LYP/6-31G* level of theory have been carried out for **1**. As expected, a twisted boat conformation of the central six-membered ring Sn_3S_3, see Fig. 7, is obtained as the global minimum, similar to the geometry found in the crystal structure of **1**. Only the orientation of the phenyl rings differs slightly as a result of crystal packing effects. Additionally a chair conformation, also depicted in Fig. 7, could be localized. The vibrational analysis yielded one negative vibration of $-7.9i$ cm^{-1}. This vibration corresponds to a rotation of one of the phenyl rings and may be related to the limited accuracy of the calculation at this level. Furthermore an only slightly twisted boat conformation has been calculated which is only by 3.4 kJ mol^{-1} higher in its total energy than the global minimum. However, this conformer slowly turns into the twisted boat conformation during optimization and cannot be regarded as a minimum. But this structure gives an idea of the energy differences caused by the three possible conformations of the central six-membered ring.

The geometry (bond lengths, bond angles, dihedral angles) of the Sn_3S_3 ring in the three calculated conformations of **1** are summarized in Tables 6–8.

The calculated geometry of twist-boat-**1** is in good agreement with the data of the crystal structure analysis however the calculated Sn–S bonds are in average 0.02 8 Å longer and the angles Sn–S–Sn are 2–4° larger. The dihedral angles of a six-membered ring follow the sequence 0, $+\varphi$, $-\varphi$, 0, $+\varphi$, $-\varphi$ in a boat conformation and the sequence $+\varphi$, $-\varphi$, $+\varphi$, $-\varphi$, $+\varphi$, $-\varphi$ in a chair conformation, which can be approximated from the values in Table 8.

Table 1
^{77}Se-, ^{125}Te- and ^{119}Sn-NMR chemical shifts (ppm) and coupling constants (Hz) of $(Ph_2SnE)_3$ (**1**–**3**)

	E	δ_E	δ_{Sn}	$^1J_{SnE}$	$^2J_{119Sn117Sn}$
1	S	–	18	–	215
2	Se	−436	−43	1324	238
3	Te	−991	−201	3369	252

Table 2
^{13}C- and ^{1}H-NMR chemical shifts (ppm) and Sn–C coupling constants (Hz) of **1**–**3**

	E	δ_C								δ_H	
		ipso	$^1J_{SnC}$	*ortho*	$^2J_{SnC}$	*meta*	$^3J_{SnC}$	*para*	$^4J_{SnC}$	*ortho*	*meta+para*
1	S	140.6	632	135.4	53	128.7	71	129.8	15	7.51	7.26
2	Se	140.0	580	135.5	53	128.6	67	129.7	14	7.48	7.28
3	Te	137.5	486	135.6	51	128.5	62	129.4	15	7.46	7.15

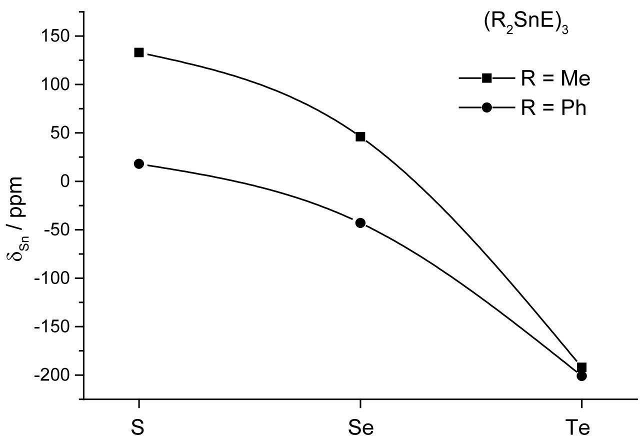

Fig. 1. ^{119}Sn-NMR chemical shift in $(R_2SnE)_3$ as a function of the element E (S, Se, Te) for R = Me [15] and Ph (**1**–**3**).

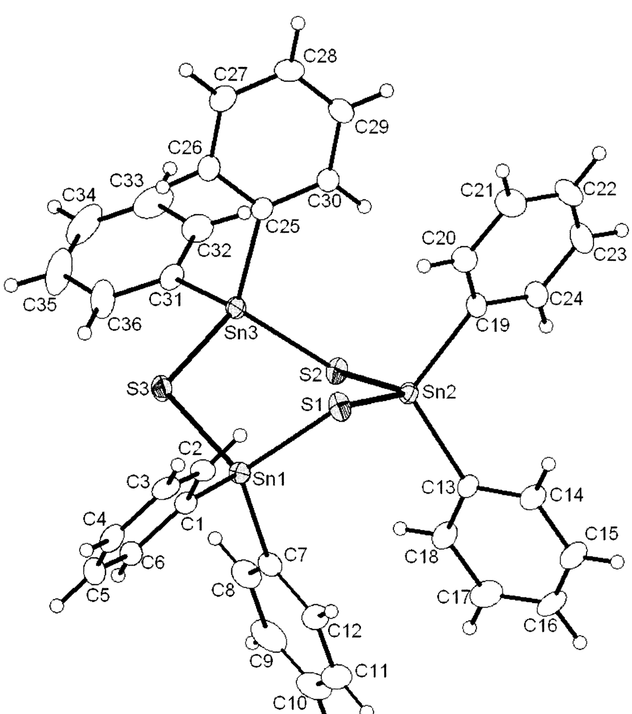

Fig. 2. ORTEP plot of the molecular structure of **1**.

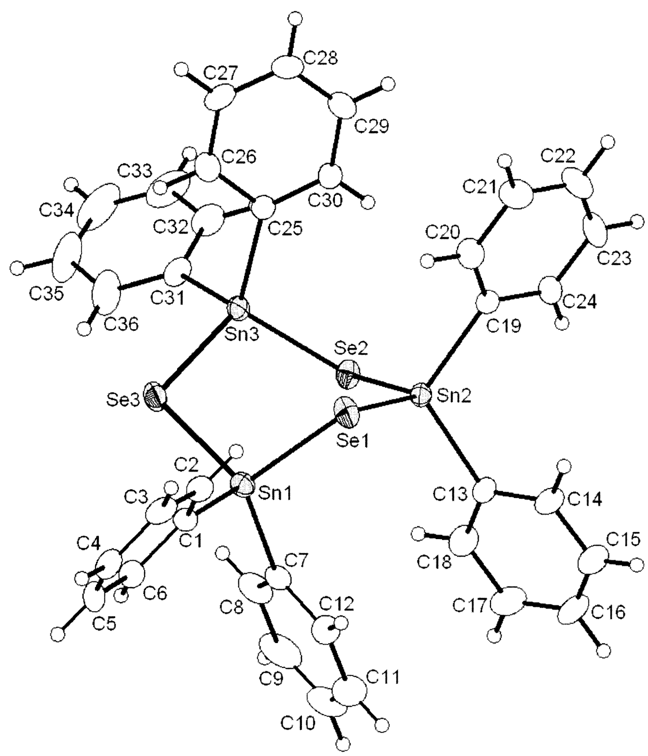

Fig. 3. ORTEP plot of the molecular structure of **2**.

3. Experimental

3.1. NMR spectroscopy

All NMR spectra were recorded on a Bruker DPX 400 in $CDCl_3$ solution and TMS as internal standard for ^{1}H and ^{13}C. ^{77}Se, ^{125}Te and ^{119}Sn spectra were recorded using an igated pulse program. External Me_4Sn, Ph_2Se_2 (δ_{Se}: 460 ppm) Ph_2Te_2 (δ_{Te}: 422 ppm) in $CDCl_3$ were used as standards for ^{119}Sn ^{77}Se and ^{125}Te.

3.2. Crystal structure analyses

X-ray structure analyses measurements were performed on a Bruker SMART CCD. Crystal data of **1**–**3** as well as data collection and refinement details are given in Table 9.

The unit cells were determined with the program smart [17]. For data integration and refinement of the

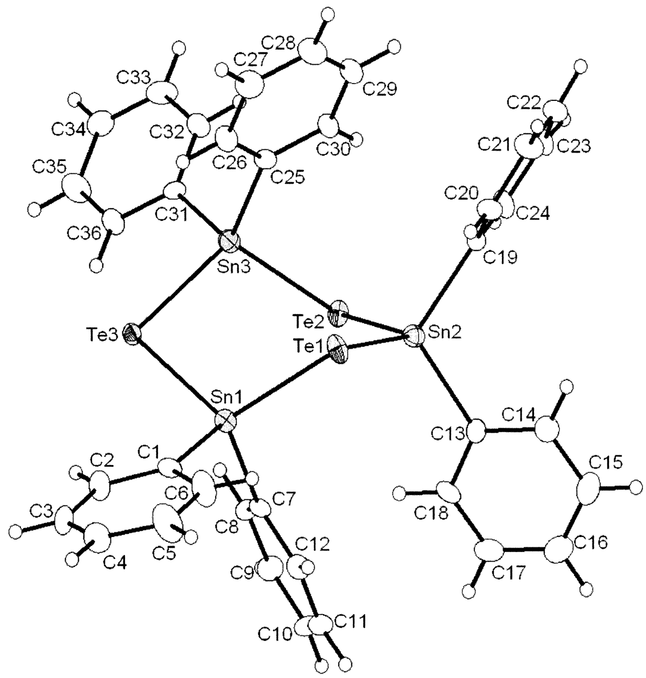

Fig. 4. ORTEP plot of the molecular structure of **3**.

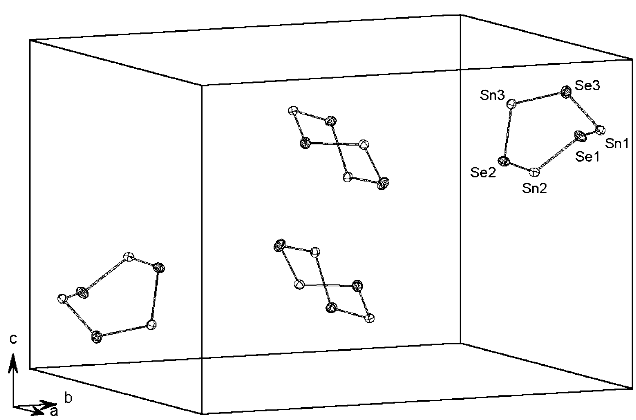

Fig. 5. Orientation of the four molecules of **2** in the unit cell. The carbon and hydrogen atoms are omitted for clarity. Compound **1** crystallizes isomorphously yielding an almost identical picture.

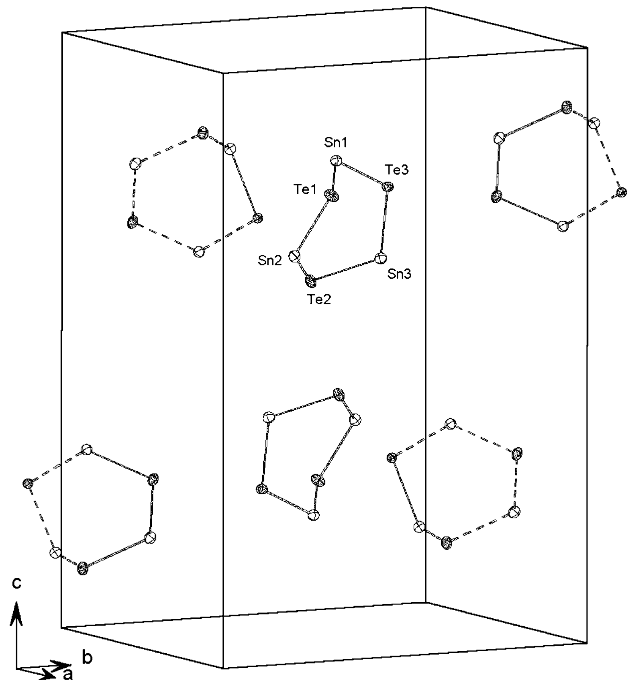

Fig. 6. Orientation of the molecules of **3** in the unit cell. Dashed bonds connect atoms outside the drawn unit cell. The carbon and hydrogen atoms are omitted for clarity.

Table 3
Selected bond distances (Å) of **1**–**3**

Atoms	**1** (E = S)	**2** (E = Se)	**3** (E = Te)
Sn(1)–E(1)	2.402(1)	2.520(1)	2.725(1)
Sn(1)–E(3)	2.408(1)	2.538(1)	2.734(1)
Sn(2)–E(1)	2.401(1)	2.521(1)	2.738(1)
Sn(2)–E(2)	2.425(1)	2.546(1)	2.740(1)
Sn(3)–E(2)	2.400(1)	2.521(1)	2.720(1)
Sn(3)–E(3)	2.399(1)	2.521(1)	2.730(1)
Sn(1)–C(1)	2.128(3)	2.132(5)	2.143(8)
Sn(1)–C(7)	2.130(3)	2.137(5)	2.118(7)
Sn(2)–C(13)	2.118(3)	2.121(5)	2.148(8)
Sn(2)–C(19)	2.131(3)	2.139(5)	2.127(8)
Sn(3)–C(25)	2.136(3)	2.133(5)	2.150(8)
Sn(3)–C(31)	2.134(3)	2.149(5)	2.146(8)

Table 4
Bond angles (°) of the central six-membered ring of **1**–**3**

Atoms	**1** (E = S)	**2** (E = Se)	**3** (E = Te)
E(1)–Sn(1)–E(3)	109.67(3)	111.74(3)	115.93(3)
E(1)–Sn(2)–E(2)	111.90(3)	113.71(2)	115.48(3)
E(2)–Sn(3)–E(3)	111.91(8)	112.95(2)	113.14(3)
Sn(1)–E(1)–Sn(2)	103.56(3)	101.15(3)	98.69(3)
Sn(2)–E(2)–Sn(3)	105.69(3)	103.11(3)	97.74(4)
Sn(1)–E(3)–Sn(3)	104.96(3)	101.68(2)	95.82(3)

unit cells the program SAINT [17] was used. The space groups were determined using the programs XPREP [17]. All data were corrected for absorption using SADABS [18]. The structures were solved using direct methods (SIR-97 [19]), refined using least-squares-methods (SHELX-97 [20]) and drawn using DIAMOND [21]. The ellipsoides at the nonhydrogen atoms are shown at the 50% probability level.

3.3. DFT calculations

The ab initio molecular orbital calculations of **1** were carried out using the GAUSSIAN-98 series of programs [22]. Geometries were fully optimized at the density functional theory level (DFT), using Becke's three-parameter hybrid exchange functional and the correlation functional of Lee, Yang and Parr (B3LYP) [23,24].

Table 5
Dihedral angles (°) of **1**–**3**

Atoms	**1** (E = S)	**2** (E = Se)	**3** (E = Te)
Sn(1)–E(1)–Sn(2)–E(2)	36.99(4)	35.39(3)	34.88(4)
E(1)–Sn(2)–E(2)–Sn(3)	29.56(4)	30.35(3)	29.64(4)
Sn(2)–E(2)–Sn(3)–E(3)	−71.26(4)	−74.09(3)	−83.18(4)
E(2)–Sn(3)–E(3)–Sn(1)	33.73(4)	36.24(3)	48.06(3)
Sn(3)–E(3)–Sn(1)–E(1)	39.39(4)	40.48(4)	35.02(3)
E(3)–Sn(1)–E(1)–Sn(2)	−78.13(4)	−79.02(4)	−77.93(4)

Table 6
Calculated bond distances (Å) of the three conformers of **1**

Atoms	Twisted boat	Boat	Chair
Sn(1)–S(1)	2.434	2.429	2.428
Sn(1)–S(3)	2.432	2.430	2.437
Sn(2)–S(1)	2.437	2.438	2.436
Sn(2)–S(2)	2.438	2.431	2.428
Sn(3)–S(2)	2.433	2.432	2.434
Sn(3)–S(3)	2.433	2.436	2.427
Average	2.434	2.433	2.432

Table 7
Calculated bond angles (°) of the three conformers of **1**

Atoms	Twisted boat	Boat	Chair
S(1)–Sn(1)–S(3)	111.4	112.7	113.1
S(1)–Sn(2)–S(2)	110.7	111.6	112.6
S(2)–Sn(3)–S(3)	110.9	111.9	113.6
Sn(1)–S(1)–Sn(2)	107.8	108.2	111.5
Sn(2)–S(2)–Sn(3)	108.0	109.7	111.8
Sn(1)–S(3)–Sn(3)	107.2	108.7	112.0

Table 8
Calculated dihedral angles (°) of the three conformers of **1**

Atoms	Twisted boat	Boat	Chair
Sn(1)–S(1)–Sn(2)–S(2)	+33.8	+9.0	−53.4
S(1)–Sn(2)–S(2)–Sn(3)	+31.1	−61.8	+52.5
Sn(2)–S(2)–Sn(3)–S(3)	−71.5	+51.8	−51.2
S(2)–Sn(3)–S(3)–Sn(1)	+36.0	+7.7	+50.3
Sn(3)–S(3)–Sn(1)–S(1)	+32.3	−62.5	−51.1
S(3)–Sn(1)–S(1)–Sn(2)	−70.8	+52.9	+52.7

Geometry optimizations, harmonic frequencies, and zero-point vibrational energies were calculated with the polarized 6-31G* basis set for C, H and S [25,26] and with effective core potentials for Sn [27]. Twist-boat **1** has a total energy of −2594.717999 H and a zero-point vibrational energy of 0.549297 H, for the chair conformation of **1** we found a total energy of −2594.714964 H and a zero-point vibrational energy of 0.549170 H. For the boat conformation we stopped the optimization at a total energy of −2594.716718 H. Further optimization led to the twist-boat conformer of **1**.

3.4. Starting materials

S, Se, 1 M Li[BEt_3H] in THF (super hydride) and Ph_2SnCl_2 were commercially available. THF was distilled from sodium potassium alloy prior to use. The other solvents were dried over KOH or sodium wire. All reactions were carried out under argon applying standard Schlenk techniques.

3.5. Preparation of (Ph_2SnE)$_3$ (**1**–**3**)

E (S, Se, Te, 2 mmol) was dissolved in 4 ml of a 1 M solution of Li[BEt_3H] in THF forming a Li_2E solution.

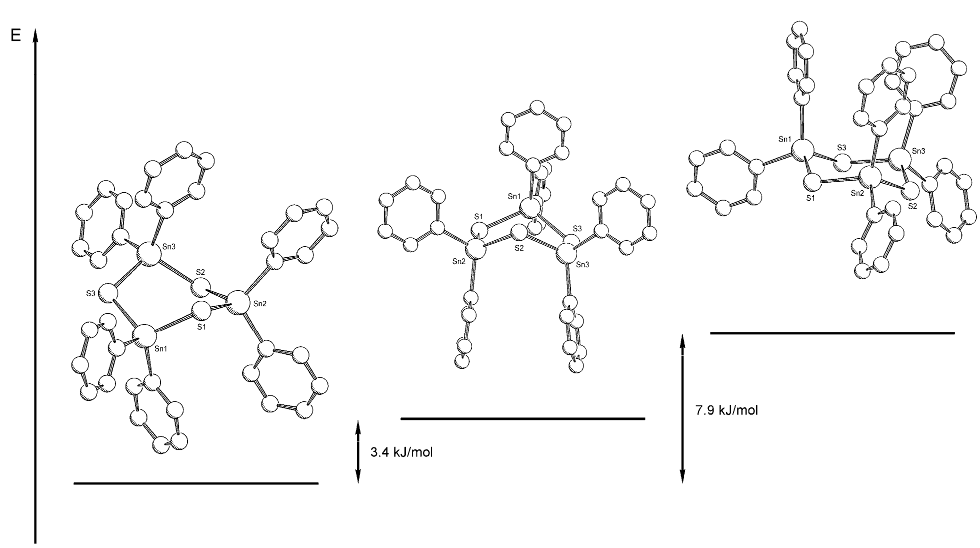

Fig. 7. Geometries and relative total energies of the three calculated conformations of **1**. The hydrogen atoms are omitted for clarity.

Table 9
Crystal data of **1**–**3** as well as data collection and refinement details

	1	**2**	**3**
Empirical formula	$C_{36}H_{30}S_3Sn_3$	$C_{36}H_{30}Se_3Sn_3$	$C_{36}H_{30}Sn_3Te_3$
Crystal shape	Block	Block	Flat rod
Crystal color	Colorless	Colorless	Yellow
Crystal size (mm)	0.40 × 0.30 × 0.20	0.40 × 0.30 × 0.20	0.30 × 0.08 × 0.04
Formula weight	914.85	1055.55	1201.47
Crystal system	Monoclinic	Monoclinic	Monoclinic
Space group	$P2_1/n$	$P2_1/n$	$P2_1/n$
Unit cell dimensions			
a (Å)	12.104(3)	12.133(4)	10.182(4)
b (Å)	21.611(4)	22.066(7)	16.423(6)
c (Å)	13.542(3)	13.649(4)	21.939(8)
β (°)	94.940(5)	95.63(1)	93.819(8)
V (Å^3)	3529.3(12)	3637(2)	3660(2)
Z	4	4	4
D_{calc} (g cm^{-3})	1.722	1.928	2.180
Linear absorption coefficient (mm^{-1})	2.307	5.070	4.398
T (K)	173(2)	173(2)	173(2)
Scan method	ω scans	ω scans	ω scans
Absorption correction	Empirical	Empirical	Empirical
Max./min. transmission	0.6554/0.4588	0.4304/0.2363	0.8437/0.3521
Measured reflections	17549	18012	18164
Independent reflections	8917	8342	10352
Observed reflections	7014	5463	5631
R_{int}	0.0257	0.0492	0.0575
θ Range for collection (°)	1.78–30.92	1.76–31.02	1.55–30.93
Index ranges	$-12 \leq h \leq 17$, $-14 \leq k \leq 30$, $-18 \leq l \leq 15$	$-15 \leq h \leq 16$, $-5 \leq k \leq 31$, $-15 \leq l \leq 13$	$-4 \leq h \leq 14$, $-10 \leq k \leq 23$, $-31 \leq l \leq 31$
Completeness to θ_{max} (%)	79.7	71.8	89.3
Final R_1/wR^2 [a] ($I > 2\sigma(I)$)	0.0297/0.0610	0.0381/0.0669	0.0469/0.0873
Final R_1/wR^2 [a] (all data)	0.0443/0.0652	0.0777/0.0764	0.1187/0.1065
Goodness-of-fit (S) [b] on F^2	0.977	0.936	0.919
H-locating and refining	Geom./constr.	Geom./constr.	Geom./constr.
Max./min. electron density (e Å^{-3})	0.438/−0.783	0.656/−0.600	1.243/−1.136

[a] $R_1 = \Sigma(||F_o|-|F_c||)/\Sigma|F_o|$, $wR^2 = [\Sigma(w(F_o^2-F_c^2)^2)/\Sigma(wF_o^2)]^{1/2}$, $w = 1/[\sigma^2(F_o^2)+(aP)^2+bP]$ where $P = (F_o^2+2F_c^2)/3$.
[b] $S = [\Sigma\ w(F_o^2-F_c^2)^2]/(n-p)^{1/2}$, n = used reflections, p = used parameters.

Ph_2SnCl_2 (2 mmol, 0.69 g) was dissolved in 1 ml toluene and added to the Li_2E solution. After stirring overnight the solvents were removed in vacuo and replaced by 10 ml toluene. After filtration from precipitated lithium salts the solvent was removed in vacuo yielding **1**–**3** as crystalline residues in approximately 70% yield which then were recrystallized from toluene/hexane mixtures to give single crystal suitable for X-ray analysis.

4. Supplementary material

Crystallographic data (excluding structural factors) for the structural analysis have been deposited with the Cambridge Crystallographic Data Centre, CCDC nos. 185227 (**1**), 185228 (**2**) and 185229 (**3**). Copies of this information may be obtained free of charge from The Director, CCDC, 12 Union Road, Cambridge CB2 1EZ, UK (Fax: +44-1223-336033; e-mail: deposit@ccdc.cam.ac.uk or www: http://www.ccdc.cam.ac.uk).

Acknowledgements

The authors thank the Deutsche Forschungsgemeinschaft for financial support. Special thanks are given to the Computing Centre of the TU Bergakademie Freiberg for supplying disk space and computing time. Furthermore, the authors thank Professor H. Lang, Chair of the Inorganic Chemistry, TU Chemnitz for the access to the X-ray facility used to determine the single crystal structures.

References

[1] S.R. Bahr, P. Boudjouk, G.J. McCarthy, Chem. Mater. 4 (1992) 383.
[2] Gmelin Handbuch der Anorg. Chem., Zinn, 8th ed., vol. C2, Springer-Verlag, Heidelberg, 1975.
[3] H.-J. Jacobsen, B. Krebs, J. Organomet. Chem. 136 (1977) 333.
[4] M. Dräger, A. Blecher, J. Organomet. Chem. 161 (1978) 319.
[5] A. Blecher, M. Dräger, Angew. Chem. 91 (1979) 740.
[6] H. Puff, R. Gattermayer, R. Hundt, R. Zimmer, Angew. Chem. 89 (1977) 556.
[7] B. Mathiasch, Z. Anorg. Allg. Chem. 432 (1977) 269.
[8] M. Dräger, B. Mathiasch, Z. Anorg. Allg. Chem. 470 (1980) 45.
[9] E. Tiekink, Main Group Metal Chem. 16 (1993) 65.
[10] H. Berwe, A. Haas, Chem. Ber. 120 (1987) 1175.
[11] A.J. Edwards, B.F. Hoskins, Acta Crystallogr. Sect. C 46 (1990) 1397.
[12] B.M. Schmidt, M. Dräger, J. Organomet. Chem. 399 (1990) 63.
[13] L. Pazdernik, F. Brisse, R. Rivest, Acta Crystallogr. Sect. B 33 (1977) 1780.
[14] A. Blecher, B. Mathiasch, J. Organomet. Chem. 184 (1980) 175.
[15] U. Herzog, G. Rheinwald, J. Organomet. Chem. 627 (2001) 23.
[16] M. O'Keeffe, N.E. Brese, J. Am. Chem. Soc. 113 (1991) 3226.
[17] Bruker AXS Inc., Madison, WI, 1998.
[18] Area-Detector Absorption Correction, Siemens Industrial Automation Inc., Madison, WI, 1996.
[19] A. Altomare, M.C. Burla, M. Camalli, G.L. Cascarano, C. Giacovazzo, A. Guagliardi, A.G.G. Moliterni, G. Polidori, R. Spagna, J. Appl. Crystallogr. 32 (1999) 115.
[20] G.M. Sheldrick, shelx-97. Programs for Crystal Structure Analysis (Release 97-2), University of Göttingen, Germany, 1997.
[21] M. Berndt, K. Brandenburg, H. Putz, diamond 2.1: Crystal Impact GbR, www.crystalimpact.de, Bonn, Germany, 1999.
[22] M.J. Frisch, G.W. Trucks, H.B. Schlegel, G.E. Scuseria, M.A. Robb, J.R. Cheeseman, V.G. Zakrzewski, J.A. Montgomery, Jr., R.E. Stratmann, J.C. Burant, S. Dapprich, J.M. Millam, A.D. Daniels, K.N. Kudin, M.C. Strain, O. Farkas, J. Tomasi, V. Barone, M. Cossi, R. Cammi, B. Mennucci, C. Pomelli, C. Adamo, S. Clifford, J. Ochterski, G.A. Petersson, P.Y. Ayala, Q. Cui, K. Morokuma, D.K. Malick, A.D. Rabuck, K. Raghavachari, J.B. Foresman, J. Cioslowski, J.V. Ortiz, B.B. Stefanov, G. Liu, A. Liashenko, P. Piskorz, I. Komaromi, R. Gomperts, R.L. Martin, D.J. Fox, T. Keith, M.A. Al-Laham, C.Y. Peng, A. Nanayakkara, C. Gonzalez, M. Challacombe, P.M.W. Gill, B. Johnson, W. Chen, M.W. Wong, J.L. Andres, C. Gonzalez, M. Head-Gordon, E.S. Replogle, and J.A. Pople, Gaussian-98, Revision A.6, Gaussian Inc., Pittsburgh, PA, 1998.
[23] A.D. Becke, J. Chem. Phys. 98 (1993) 5648.
[24] P.J. Stevens, F.J. Devlin, C.F. Chablowski, M.J. Frisch, J. Phys. Chem. 98 (1994) 11623.
[25] P.C. Hariharan, J.A. Pople, Theor. Chim. Acta 28 (1973) 213.
[26] M.M. Francl, W.J. Petro, W.J. Hehre, J.S. Binkley, M.S. Gordon, D.J. DeFrees, J.A. Pople, J. Chem. Phys. 77 (1982) 3654.
[27] W.R. Wadt, P.J. Hay, J. Chem. Phys. 82 (1985) 284.